Anuário do Instituto de Geociências - UFRJ
https://revistas.ufrj.br/index.php/aigeo

Filling Materials in Brittle Structures as Indicator of Cenozoic Tectonic Events in Southeastern Brazil

Materiais de Preenchimento em Estruturas Rúpteis como Indicador de Eventos Tectônicos Cenozoicos no Sudeste do Brasil

Salomão Silva Calegari[1]; Thaís Ruy Aiolfi[2]; Mirna Aparecida Neves[3]; Caroline Cibele Vieira Soares[3]; Rodson de Abreu Marques[3] & Fabrício de Andrade Caxito[1]

[1] *Universidade Federal de Minas Gerais, Instituto de Geociências, Centro de Pesquisa Professor Manoel Teixeira da Costa, Programa de Pós-graduação em Geologia, Campus Pampulha, Av. Antônio Carlos, 6627, 31270-901, Belo Horizonte, MG, Brazil*

[2] *Universidade Estadual do Norte Fluminense Darcy Ribeiro, Centro de Ciência e Tecnologia, Programa de Pós-graduação em Ciências Naturais, Campus Leonel Brizola, Av. Alberto Lamego, 2000, Parque Califórnia, 28013-602, Campos dos Goytacazes, RJ, Brazil*

[3] *Universidade Federal do Espírito Santo, Departamento de Geologia, Campus Alegre, Alto Universitário, s/n, Guararema, 29500-000, Alegre, ES, Brazil*

E-mails: salomaocalegari@hotmail.com; thais.ruy@hotmail.com; mirnaan@gmail.com; carolinecvsoares@gmail.com; rodsonabreu@gmail.com; facaxito@yahoo.com.br

DOI: http://doi.org/10.11137/2020_2_237_254; Recebido: 06/11/2019 Aceito: 11/05/2020

Abstract

The filling materials in brittle structures can provide useful information about the Cenozoic evolution developed over proterozoic terrains. When these materials are affected by faults, they record deformation phases that can be determined chronologically and, in the occurrence of lateritic materials, it is possible to infer the paleoenvironmental conditions during the mineral formation. This work aimed to identify crystalline phases of brittle structure filling materials and to propose evolutionary interpretations for Cenozoic tectonic reactivation based on literature data. The study area is located in the Southern part of the Espírito Santo State, near the Brazilian Southeastern Continental Margin, where proterozoic geological structures have been reactivated since the mesozoic rift phase, up to the Holocene. The mineral assemblage found in the filling materials includes primary minerals such as quartz, muscovite, microcline, rutile, titanite, and bannisterite; and the weathering minerals such as kaolinite, illite, hematite, goethite, hydrobiotite, lithiophorite and, birnessite. The mineralogical association found in the filling materials denotes the action of fluid phases with mineral precipitation at the brittle discontinuities during the weathering processes that occurred during the Cenozoic, probably between the Miocene and the Pleistocene. The faults, which striations are marked on the filling materials, originated after (in the case of the manganese oxides) or during (in the case of the illite) the mineral formation, indicating that the maximum age of these faults is in the Miocene. The origin of the brittle structures that affected the filling materials studied here is linked to the uplifting of the Continental Brazilian Margin, when ancient geological structures were reactivated as normal faults due to the local action of an extensional regime.

keywords: Brittle Structures; Relative Dating; Cenozoic.

Resumo

Os materiais de preenchimento de estruturas rúpteis podem fornecer informações importantes sobre a evolução cenozoica em terrenos proterozoicos. Quando afetados por falhas, eles permitem determinar cronologicamente as fases de deformação e, quando materiais lateríticos ocorrem, é possível definir as condições paleoambientais durante a formação dos minerais. O objetivo deste trabalho é identificar as fases cristalinas dos materiais de preenchimento de estruturas rúpteis e propor interpretações evolutivas quanto à reativação tectônica cenozoica com base nos dados da literatura. A área de estudos é a porção Sul do Estado do Espírito Santo, nas proximidades da Margem Continental do Sudeste do Brasil, onde estruturas geológicas proterozoicas têm sido reativadas desde a fase rifte mesozoica até o Holoceno. A assembleia mineral encontrada nos materiais de preenchimento inclui os minerais primários: quartzo, muscovita, microclina, rutilo, titanita e banisterita; além dos minerais de intemperismo: caolinita, ilita, hematita, goethita, hidrobiotita, litioforita e birnessita. A associação mineralógica encontrada nos materiais de preenchimento denota a ação das fases fluidas com precipitação mineral em descontinuidades rúpteis durante os processos de intemperismo que ocorreram durante o Cenozoico, provavelmente entre o Mioceno e o Pleistoceno. As falhas, com estrias marcadas nos materiais de preenchimento, originaram-se depois (no caso dos óxidos de manganês) ou durante (no caso da ilita) a formação mineral, indicando idade máxima dessas falhas no Mioceno. A origem das estruturas rúpteis que afetaram os materiais de preenchimento aqui estudados está ligada ao soerguimento da Margem Continental Brasileira, quando estruturas geológicas herdadas foram reativadas como falhas normais devido à ação de um regime distensional local.

Palavras-chave: Estruturas Rúpteis; Datação Relativa; Cenozoico.

1 Introduction

The mobilization of material through the weathering profile, carrying substances to a deeper level of the substrate, can occur along discontinuities, where mineral precipitation is favored. These discontinuities generally are brittle structures, such as joints and faults, which control fluid flow in low permeable rocks. Depending on their nature, distribution, continuity, and connectivity, these structures allow the transport of mineralizing fluids (Kurz *et al*., 2008; Faulkner *et al*., 2010; Balsamo *et al*., 2013), as they generate ducts and sites for mixing of fluids and mineral precipitation (Zhang *et al*., 2008).

The study of weathering profiles and lateritic materials can help understand the Cenozoic geological events, as they give information about climate and relief evolution, environmental conditions, weathering intensity, and Neotectonic phases (Costa, 1991; Romano & Castañeda, 2006; Santos & Ladeira, 2006; Modenesi-Gauttieri *et al*., 2011; Augustin *et al*., 2013). Here, we use the term laterite as referring to the weathering material composed mainly by oxides and hydroxides of Aluminum and Iron, clay minerals and some silicates, commonly originated under hot and wet climate (Allaby, 2008).

According to Monteiro *et al*. (2014), the rocks and laterites exposed at the atmosphere-hydrosphere-lithosphere-biosphere interface, are constantly reworked by mineral dissolution and re-precipitation. Supergene deposits with manganese oxides are formed due to strong and prolonged weathering processes, resulting in a thick cover of weathered rock under wet and hot climate, favorable geomorphologic conditions, and relatively stable tectonic environment (Deng & Li, 2013).

The compositional study of brittle structure filling material made it possible, according to Carmo & Vasconcelos (2004) and De Putter *et al.* (2015), to access information about climate, tectonic environment, and geomorphology at the time of mineral formation. Lateritic material that fills the space between the rock discontinuities is called, by Costa (1991), as "fissure ferruginous rock", that compose thin goethite laminas accumulated on the fracture walls. Some supergene manganese minerals that fill brittle structures can be dated using isotopic and paleoclimate data (Carmo & Vasconcelos, 2004; 2006; De Putter *et al*., 2015).

In the State of Espírito Santo, Southeastern Brazil, Calegari *et al*. (2016) identified brittle structures with lateritic materials and clay minerals that fill or cover planar joint and fault surfaces. The mineralogical characterization of these materials can give relevant information about the poorly understood Cenozoic tectonic evolution and weathering processes of this region.

In this work, we selected eight outcrops where brittle structures with filling material occur, seven of them located in Southern Espírito Santo and one in the Southeastern of Minas Gerais State (Figure 1). The aim is to identify the crystalline phases of filling materials and analyze the structures for kinematic interpretations of the Cenozoic tectonic tying up with literature data.

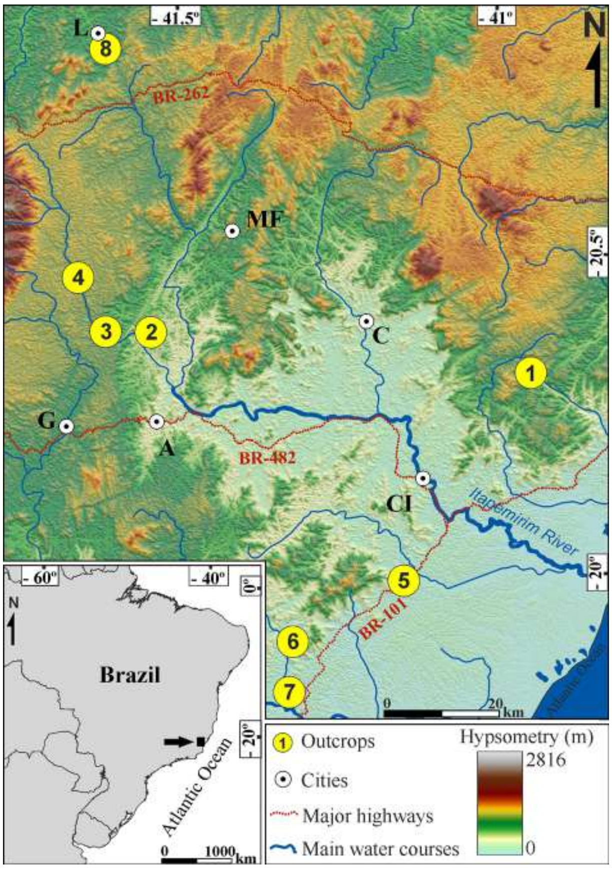

Figure 1 Outcrops location map. Cities: A = Alegre, C = Castelo, CI = Cachoeiro de Itapemirim, G = Guaçuí, L = Lajinha, MF = Muniz Freire. Vetorial map data from GEOBASES (2002).

2 Methods

During the field works, after the detailed description and photographic register of the outcrops, samples of filling materials and host rocks were collected, also the attitude of geological structures was measured. For the identification of the mineral phases, the material was analyzed macroscopically with the naked eye, with a hand magnifier (20-times magnification), and a binocular loupe (10, 15, 20, 30 and 40-times magnification). The samples with black color were submitted to the peroxide hydrogen reaction test in order to verify the eventual presence of manganese oxides.

Twenty samples were prepared for diffractometric analysis by trituration using an agate mortar, up to reach granulation minor than a 350-mesh screen (0,044 millimeters). The diffractograms were constructed using a goniometer with cooper anode x-ray tubes, K-alfa radiation with 1,45418 Angstrom wavelength, scanning speed of 0,3° 2 theta/min, and 2 theta angle varying from 5 to 75º. The diffractograms were interpreted using the software X'Pert HighScore Plus v. 2.0.1 and known patterns from the literature (Brindley & Brown, 1980).

The structural data were analyzed using the software OpenStereo v. 0.1.2f (Grohmann *et al*., 2011) and WinTensor v. 5.8.9 (Delvaux & Sperner, 2003). The joint data were plotted on density stereograms, and the fault data were inverted by the "Right Dihedron Method" (Angelier & Mechler, 1977), in order to obtain four classifications of the reduced stress tensor: the main stress axes: σ1, σ2, and σ3 (maximum, intermediate, and minimum compression) and the stress ratio R (R = σ2 - σ3 / σ1 - σ3). To obtain the stress regime, we used the values of R according to the classification defined by Delvaux *et al.* (1997): radial extensive (UF; vertical σ1, $0 < R < 0.25$); pure extensive (NF; σ1 vertical, $0.25 < R < 0.75$), transtensive (NS; σ1 vertical, $0.75 < R < 1$ or σ2 vertical, $1 < R < 0.75$); pure strike-slip (SS; σ2 vertical, $0.75 < R < 0.25$); transpressive (TS; σ2 vertical, $0.25 < R < 0$ or σ3 vertical, $0 < R < 0.25$); pure compressive (TF; σ3 vertical, $0,25 < R < 0,75$), and radial compressive (UF; σ3 vertical, $0,75 < R < 1$). Kinematic data were plotted on Frohlich's Triangular Diagram (Frohlich, 1992) to assess the distribution of the stress regime in the area. Finally, for the deformation analysis, we used the values acquired by the fault data inversion to obtain the paleotension fields by the "Rotational Optimization" procedure using the F5 function in the Win-Tensor software.

3 Geological Setting

The study area is located in the Araçuai Belt domain, Northern part of the Mantiqueira Province (Almeida *et al*., 1981; Heilbron *et al*., 2004; Fuck *et al*., 2008). The Mantiqueira Province is a segment of the Brazilian-Pan African Orogenic System developed, during the Neoproterozoic and the beginning of the Paleozoic (Almeida *et al*., 1981; Brito-Neves *et al*., 1999). The collisional event that generated this orogenic system registered in the Atlantic Margin of South America and Africa, is called Brazilian-Pan African orogeny.

The Araçuaí Belt extends between the parallels 15º e 21º south, from the eastern limit of the São Francisco Craton up to the South Atlantic Coast. The Araçuaí Belt Southern limit is considered as a transition zone where the foliation trend changes from N-S to NE-SW, near the 21º parallel, at the very beginning of the Ribeira Belt, belonging to the central segment of the Mantiqueira Province (Pedrosa Soares & Wiedemann-Leonardos, 2000).

The study area is located at the Crystalline Nucleus of the Orogenic System, comprised of a Paleoproterozoic substrate, metamorphosed in high-amphibolite to granulite facies; metasedimentary – metavolcanosedimentary assemblage (paragneiss complexes) and pre to post-collisional granitic suites (G1 to G5; Alkmim *et al*., 2006; Figure 2).

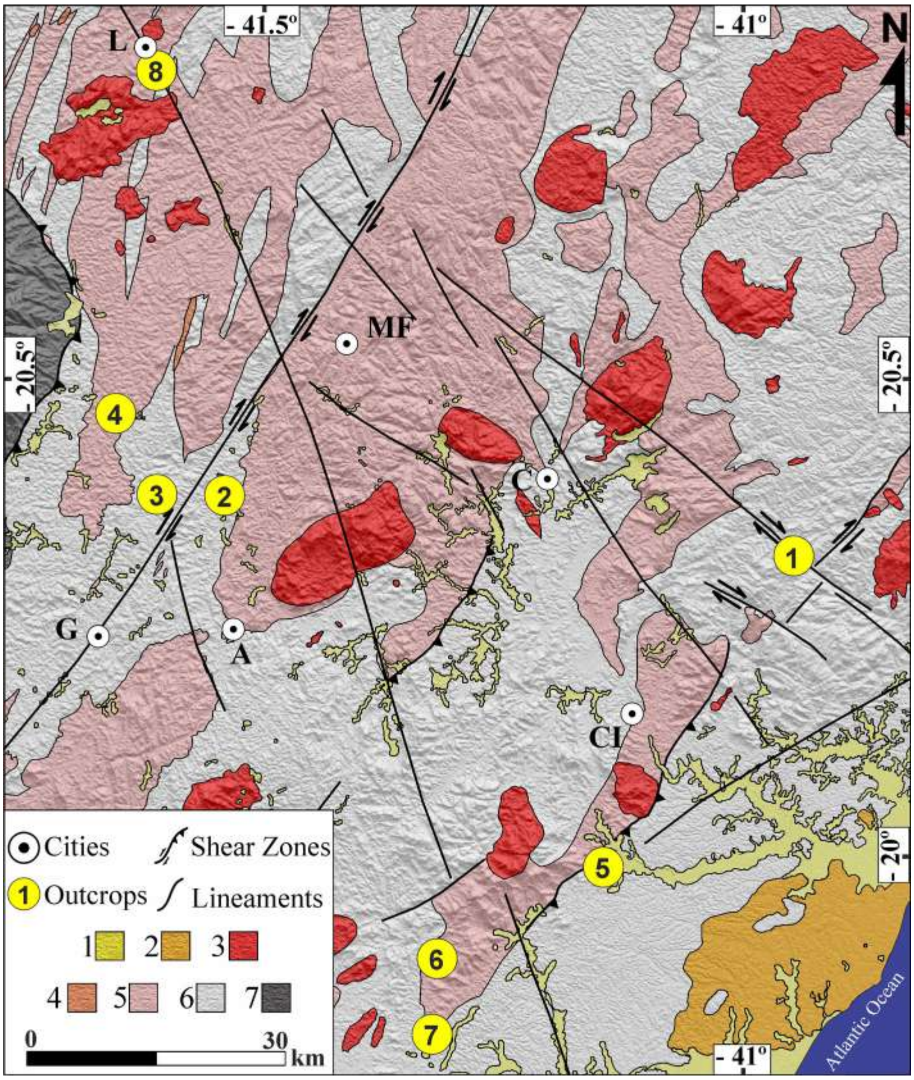

Figure 2 Regional geological map showing lithotypes and geological framework of study area (modified from Horn *et al*. (2007); Novo *et al*. (2014) and Vieira & Menezes (2015), with location of sampling outcrops. ASTER GDEM image from ERSDAC (2013). Lithological units: 1 = Alluvial-colluvial/coastal deposits, 2 = Barreiras Formation, 3 = G5 Supersuite, 4 = G2 Supersuite, 5 = G1 Supersuite, 6 = Metasedimentary and metavolcanosedimentary rocks, 7 = Basement complexes. Shear zones: G = Guaçuí, B = Batatal. Lineaments: A = Alegre, I = Itaoca, P = Piúma. Cities: A = Alegre, CI = Cachoeiro de Itapemirim, G = Guaçuí, L = Lajinha, MF = Muniz Freire, C = Castelo.

The Caparaó Suite, a Paleoproterozoic remaining unit, is a granulitic association with enderbites, charnockites, diorites, and gabbroic rocks, which occurs in the core of a large antiformal structure at the homonymous mountain range (Noce *et al*., 2007).

The metasedimentary and metavolcanosedimentary rocks, metamorphosed in the pre-orogenic stage, are aluminous gneisses derived from calcium-silicate rocks and volcano-sedimentary sequences, with basics and felsic volcanic rocks (Féboli, 1993; Pedrosa Soares *et al*., 2008). This association is included in the Paraíba do Sul Complex (Féboli, 1993) or in the Undivided Paragneisses Complex (Pedrosa Soares *et al*., 2008), and the provenance of these rocks can be related to passive margin sequences or arc complexes (Pedrosa-Soares & Wiedemann-Leonardos 2000).

The magmatic suites are 630 to 460 Ma in age, and register the various orogenic stages of the Brazilian-Pan African event (Pedrosa-Soares & Wiedemann-Leonardos, 2000; Pedrosa-Soares *et al*., 2001, 2007, 2008; Silva *et al*., 2005; Figure 2). The G1-Supersuite, pre-collisional, is related to the edification of the Araçuaí Orogen magmatic arc and is composed mainly by ortho-derivative rocks, of tonalitic and granodiorite protoliths (Pedrosa-Soares & Wiedemann-Leonardos 2000;

Pedrosa Soares *et al*., 2008; Pedrosa Soares *et al*., 2011). The G2-Supersuite, sin-collisional, is related to deformation and regional metamorphism and involves Type-S granitic protoliths, such as peraluminous, sub-alkaline, and calcium-alkaline granites (Pedrosa Soares *et al*., 2008; Pedrosa Soares *et al*., 2011). In the post-collisional stage, the plutons of G5-Supersuite formed, characterized as Type-I, with granite and charnockite, besides gabbro (De Campos *et al*., 2004; Pedrosa Soares *et al*., 2008).

The gneissic foliation, also related to the Brazilian-Pan African Cycle, has a main trend in the NE-SW to N-S striking (Wiedemann *et al*., 2002), while the mylonitic foliation occurs along the shear zones with NE-SW to NNE-SSW striking. These shear zones, such as the Guaçuí Shear Zone (GSZ) and the Batatal Shear Zone (BSZ) (Figure 2) are related to an orogenic lateral escape, at the collisional final phase (Cunningham *et al*., 1998; Alkmim *et al*., 2006).

The Alegre Lineament, with NNW-SSE striking, reflects a regional fault zone that reaches the Campos coastal basin (Calegari *et al*., 2016). It is considered of Cambrian age, but with distensive reactivation movements that occurred during the rift phase and at the Cenozoic. The Piúma Lineament, another structure that is prominent in the area, was described as a brittle shear zone, with NW-SE striking dipping to SW (Lourenço *et al*., 2016). According to these authors, it was originated in a post-Brazilian event that promoted NNE-SSW distension and was reactivated most probably in the South Atlantic opening as a normal dextral to transtensional dextral shear zone.

The Cenozoic lithostratigraphic units present in the area, are the Miocene siliciclastic sediments of the Barreiras Formation and the quaternary alluvial-coastal deposits (Silva *et al*., 2004; Vieira & Menezes, 2015; Figure 2).

In this region, there are few studies on the Meso-Cenozoic geological evolution. Relevant studies have been developed in Southeastern Brazil, indicating periods of denudation during the Late Cretaceous, at the Paleogene and the Neogene, linked to the rupture of the Gondwana and the evolution of the coastal basin (e.g. Cogné *et al*., 2012; Karl *et al*., 2013; Hackspacher *et al*., 2004). Further north of the study area, Jelinek *et al*. (2014) identified three denudation episodes at different periods: Early Cretaceous, Late Cretaceous-Paleocene, and Neogene. Other studies developed in the same region also point out episodes of denudation in the Late Cretaceous and Neogene (Morais Neto *et al*., 2009), and in the Early Cretaceous and Late Cretaceous-Paleocene (Harman *et al*., 1998). Jelinek *et al*. (2014) and Harman *et al*. (1998) associate the Early Cretaceous denudation to the changing of local base level related to rifting and initial opening of the South Atlantic Ocean. The Late Cretaceous denudation has been associated to mantle anomalies and thermal isostasy, which caused a broad crustal lifting; and the Neogene denudation may have occurred due to climatic change, with a transition to a semi-arid climate (Morais Neto *et al*., 2009; Jelinek *et al*., 2014).

4 Results

4.1 Macroscopic Analysis

In the studied outcrops, gneisses, migmatites, and mylonites predominate, with local occurrences of mafic dikes and quartz veins (Figures 2 and 3A and C). Gneisses (outcrops 1 and 4-7), migmatites (outcrop 8) and mylonites (outcrops 2 and 3) occur as weathered rocks from reddish to whitish in color. The minerals macroscopically identified in the filling materials are quartz, feldspars, white mica, biotite, white clay and, occasionally, red and orange clay. Most samples of filling materials in brittle structures developed in gneisses show manganese oxide in the form of a black clayey material, which compounds millimetric pellicles over discontinuity planes, such as foliation and fractures. Occasionally, oxide pellicles in planes show striations, indicating kinematics (Figures 4A to C).

One of the samples (outcrop 1) is from a quartz vein that contains white mica, white clay, and manganese oxide with botryoidal habit and dendritic structure; the oxide composes thin black pellicles that fill fissures (Figures 4D to F). The diabase dikes are generally weathered and occur in outcrops 1, 5, 7, and 8. Macroscopically it is possible to observe orange, red and white clays, quartz, besides feldspars and black oxide. The oxide is on discontinuity planes, mainly in the contact between the dike and the host rock and also in striated plans (Figures 4G and H).

Figure 3 Field characteristics of some studied outcrops: A. weathered gneiss (Outcrop 1, sample 1-A); quartz vein with black oxide (Sample 1-B) and diabase dike (Sample 1-D); B. Mylonitic gneiss with foliation to N10E/85SE (Outcrop 2, sample 2-B); C. Weathered gneiss (Outcrop 7).

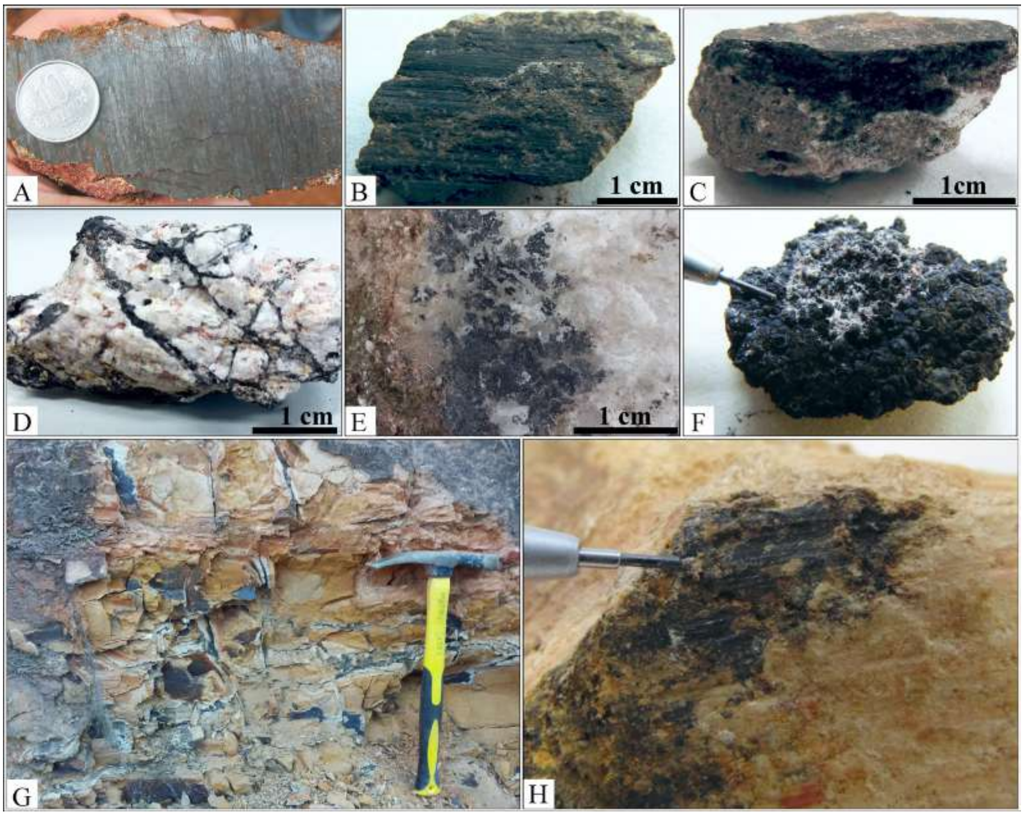

Figure 4 Manganese oxide pellicles on discontinuity planes showing fault striations: A. Sample 3-A, Outcrop 3; B. Frontal and C. lateral view of the Sample 8-A, Outcrop 8. Manganese oxides collected in quartz vein: D. filling fissures; E. composing dendritic forms and; F. showing botryoidal habit (Sample 1-B, Outcrop 1); G. Fractured diabase dike with manganese oxide filling the discontinuities (Outcrop 8) and; H. striations marked on this material (Sample 8-E).

4.2 Diffractometric Analysis

The samples analyzed by x-ray diffractometry are representative of the black and the clayey filling material in gneisses, quartz vein, and mafic dikes. The chemical composition of the primary and weathering minerals found in these samples are shown in the Tab. 1.

	Mineral	Chemical Composition
Primary Minerals	bannisterite	$KCa(Mn^{2+}, Fe^{2+}, Zn, Mg)_{20}(Si, Al)_{32}O_{76}(OH)_{16}.4\text{-}12H_2O$
	microcline	$KAlSi_3O_8$
	muscovite	$KAl_2(Si_3Al)O_{10}(OH,F)_2$
	quartz	SiO_2
	rutile	TiO_2
	titanite	$CaTiSiO_5$
Weathering Minerals	birnessite	$(Na, Ca)_{0.5}(Mn^{4+}, Mn^{3+})_2O_4.1.5H_2O$
	goethite	$\alpha\text{-}Fe^{3+}O(OH)$
	hematite	$\alpha\text{-}Fe_2O_3$
	hydrobiotite	$[K(Mg, Fe^{2+})_3(Al, Fe^{3+})Si_3O_{10}(OH, F)_2].[(Mg, Fe^{2+}, Al)_3(Si, Al)_4O_{10}(OH)_2.4H_2O]$
	illite	$(K, H_3O)(Al, Mg, Fe)_2(Si, Al)_4O_{10}[(OH)_2,(H_2O)]$
	kaolinite	$Al_2Si_2O_5(OH)_4$
	lithiophorite	$(Al, Li)Mn^{4+}O_2(OH)_2$

Table 1 Primary and weathering minerals found in the samples by XRD analysis (chemical composition from Anthony *et al.*, 2001).

In gneisses filling materials, it's observed the characteristic peaks of quartz, muscovite and microcline, and the weathering minerals kaolinite, illite, hydrobiotite, and hematite; in one of the samples, the goethite occurs, and two of them display bannisterite (Figure 5).

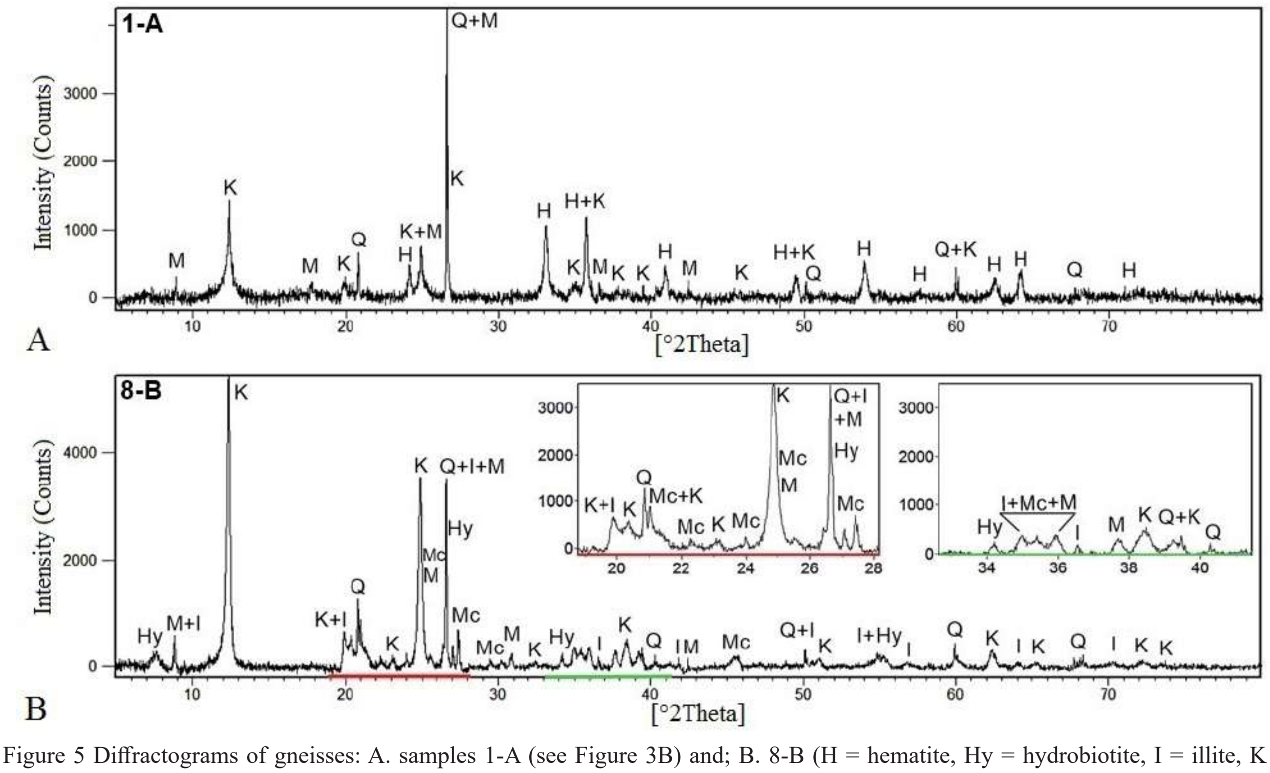

Figure 5 Diffractograms of gneisses: A. samples 1-A (see Figure 3B) and; B. 8-B (H = hematite, Hy = hydrobiotite, I = illite, K = kaolinite, Mc = microcline, M = muscovite, Q = quartz).

The kaolinite (Figures 5A and B) and illite (Figure 5B) are clay minerals common in soils (Velde & Meunier, 2008). The hydrobiotite (Figure 5B) is a phyllosilicate formed in the initial stages of weathering (Anthony *et al.*, 2001). The iron oxide and hydroxide identified in several samples are hematite (Figure 5A) and goethite. These minerals indicate different stages of iron oxidation, different humidity conditions, pH, Eh, and microbial activity during the weathering (Velde & Meunier, 2008).

The manganese minerals lithiophorite and birnessite occur on the fault planes, foliation, and fractures of gneisses (Figure 6). These minerals give a typical black color to the hand samples and are commonly associated with the presence of iron oxides (Velde & Meunier, 2008).

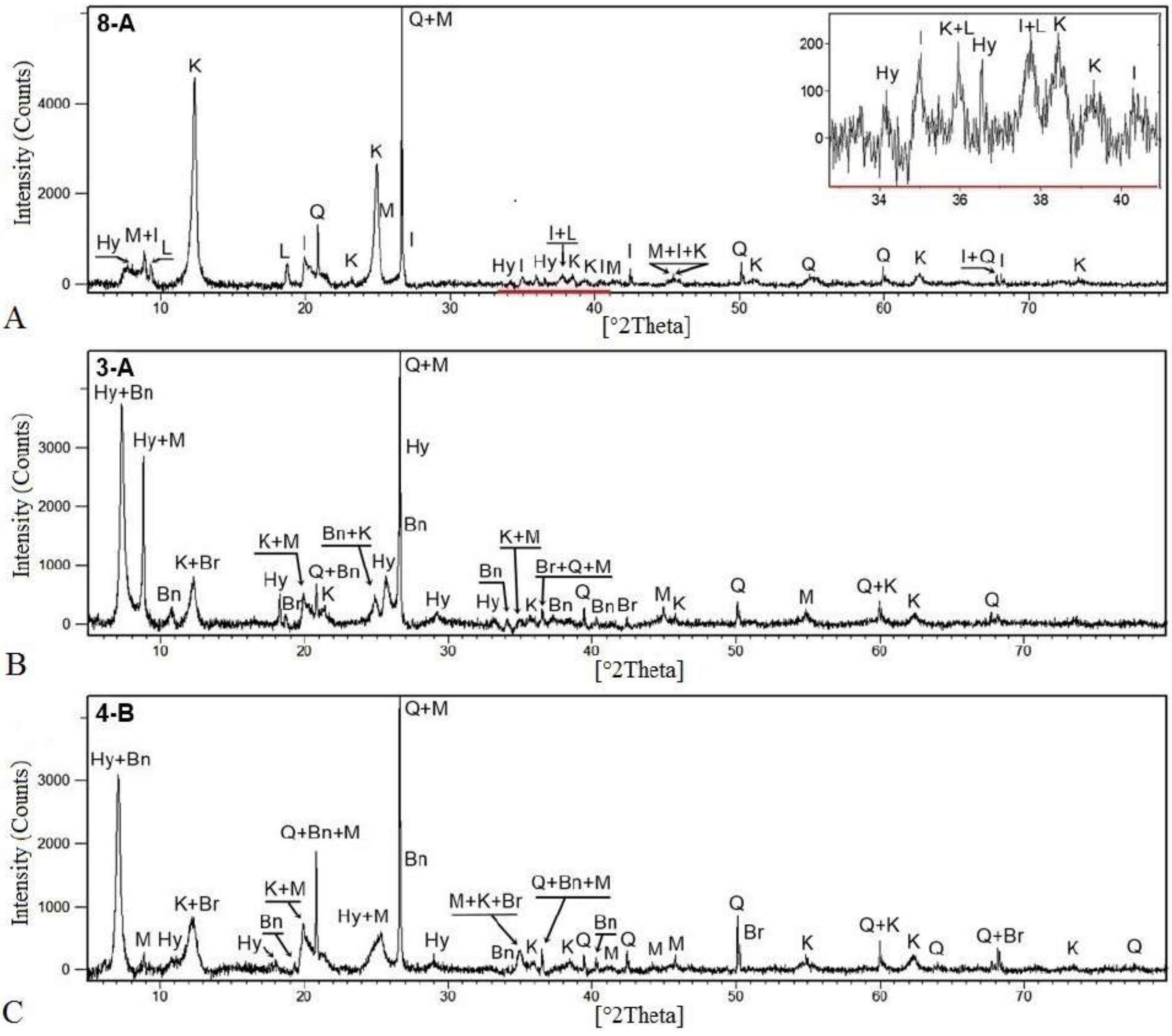

Figure 6 Diffractograms of the black filling material found on fault planes, foliation and fractures of gneisses. Samples: A. 8-A (see Figures 4B and C); B. 3-A (see Figure 4A) and C. 4-B. (Bn = bannisterite, Br = birnessite, Hy = hydrobiotite, I = illite, K = kaolinite, L = lithiophorite, M = muscovite, Q = quartz).

The bannisterite was also identified (Figures 6B and C). It is a primary mineral with the manganese as the main cation (Dunn *et al*., 1981) and occurs in manganese and zinc-bearing metamorphosed rocks (Anthony *et al*., 2001). This mineral can be related to the manganese field that occurs in the region of the Caparaó Mountain Range, according to Vieira & Menezes (2015). The other primary minerals identified are remnants that were not affected by weathering.

The quartz vein presents the peaks of quartz, muscovite, kaolinite, and lithiophorite appear (Figure 7A), while the clayey filling material in the fractures present peaks of quartz, illite, and kaolinite (Figure 7B).

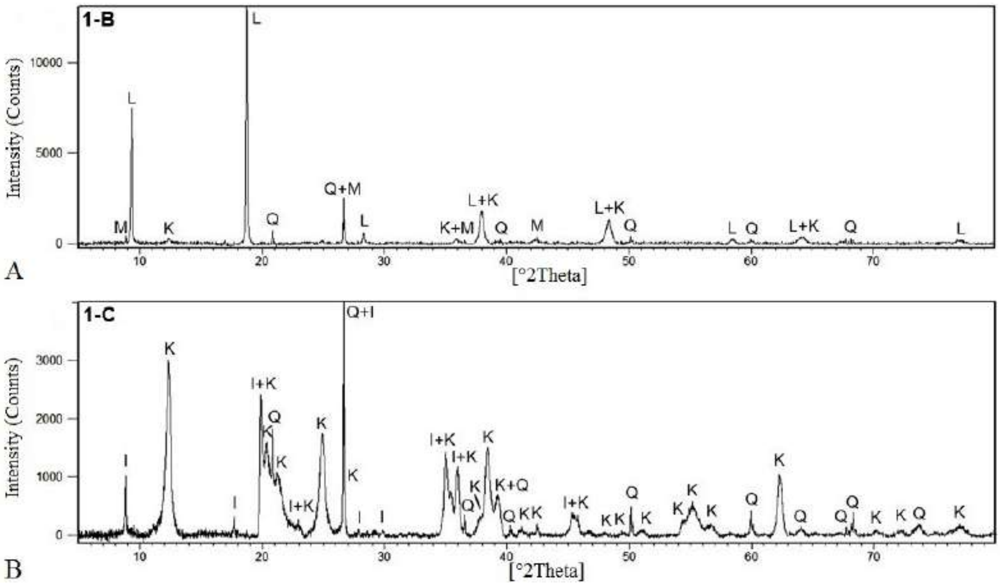

Figure 7 Diffractograms of the materials collected in the quartz vein; A. Black manganese material (sample 1-B, see Figures 3A and 4D to F) and; B. fracture filling material in the quartz vein (Sample 1-C) (I = illite; K = kaolinite; L = lithiophorite; M = muscovite; Q = quartz).

The mafic dikes have quartz, kaolinite, goethite, and titanite, (as shown in Figure 8A); besides rutile, hydrobiotite, and illite. Peaks of lithiophorite, quartz, kaolinite, goethite, illite, and hematite appear in the black filling material of striated fault planes that occur in these dikes, while the birnessite and muscovite were found in a discontinuity plane existent between the dike and the host rock (Figures 8B and C).

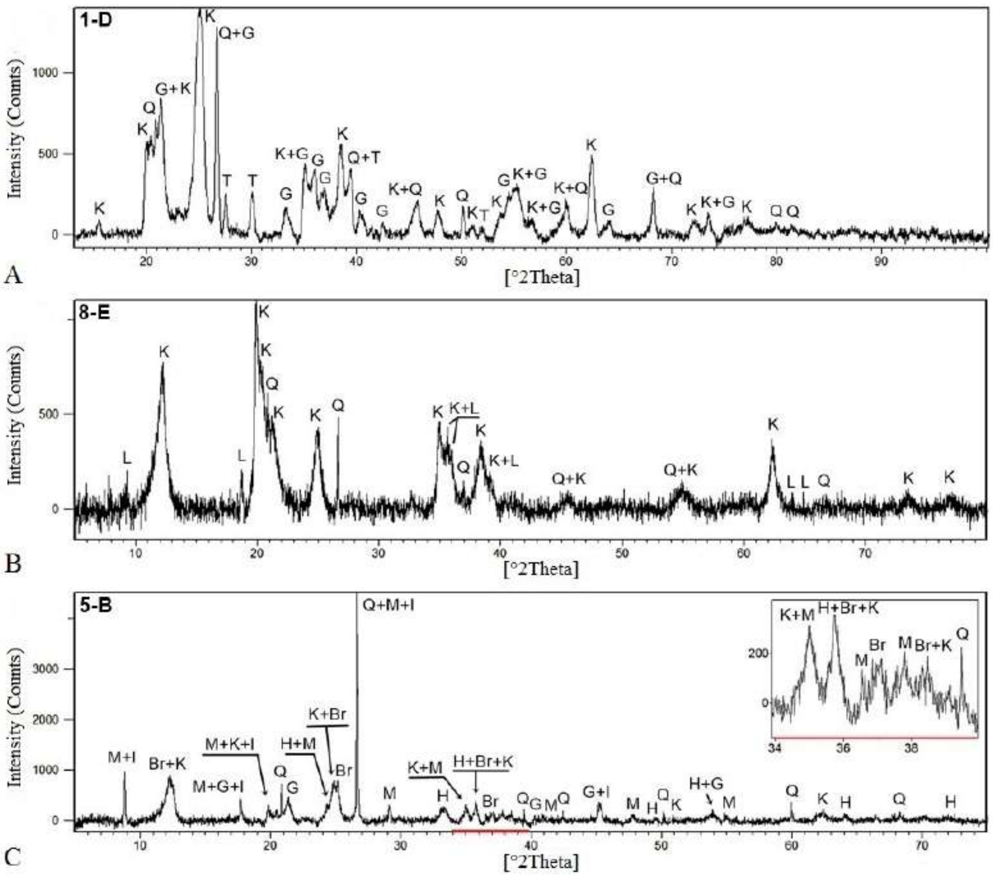

Figure 8 Diffractograms of A. mafic dike (Sample 1-D, see Figure 3A); B. and C. filling material in the mafic dike (Sample 8-E, see Figures 4G and H) and (Sample 5-B) (Br = birnessite; G = goethite; H = hematite; I = illite; K = kaolinite; L = lithiophorite; M = muscovite; T = titanite; Q = quartz).

4.3 Geological Structures and Kinematics

In the studied outcrops, 73 joints measurements and 75 brittle faults measurements were collected. The joints are distributed into three main families, one main striking NW-SE, with a high dip angle, and two other families oriented to N52E/82NW and N38W/38SW (Figure 9A). In Outcrops – 1 and 2, joints with NW-SE striking are predominant, although NE-SW striking also occurs. In Outcrop-3, there are NE-SW joints, and in Outcrops 4 and 6, preferential trends are absent.

The brittle faults occur in weathered rocks (gneisses and mafic dikes) and have fault striations marked in thin layers of the filling materials. These rupture plans are associated with normal, normal oblique and transcurrent movements; approximately 47% is related to a pure extensional tectonic regime, 23% related to a transtentional tectonic regime, 20% to a radial extensional tectonic regime, and 11% to a pure transcurrent tectonic regime (Figure 9B). The pure extensional regime is composed of mid-angle normal faults, mainly in the NE-SW and NW-SE directions, and are found in outcrops 1 to 6 and 8 (Figure 9C). Oblique faults, related to a transtensional regime, have no apparent uniform orientation and are found in outcrops 1 to 4, 6 and 8 (Figure 9D). On the other hand, normal faults that occur under the extensional radial regime have preferential NE-SW direction with a high dip angle in outcrops 2, 3, 5, and 8 (Figure 9E). The faults associated with a pure transcurrent regime, represented in outcrops 1, 2, 6, and 8, have E-W and N-S direction with a high dip angle (Figure 9F).

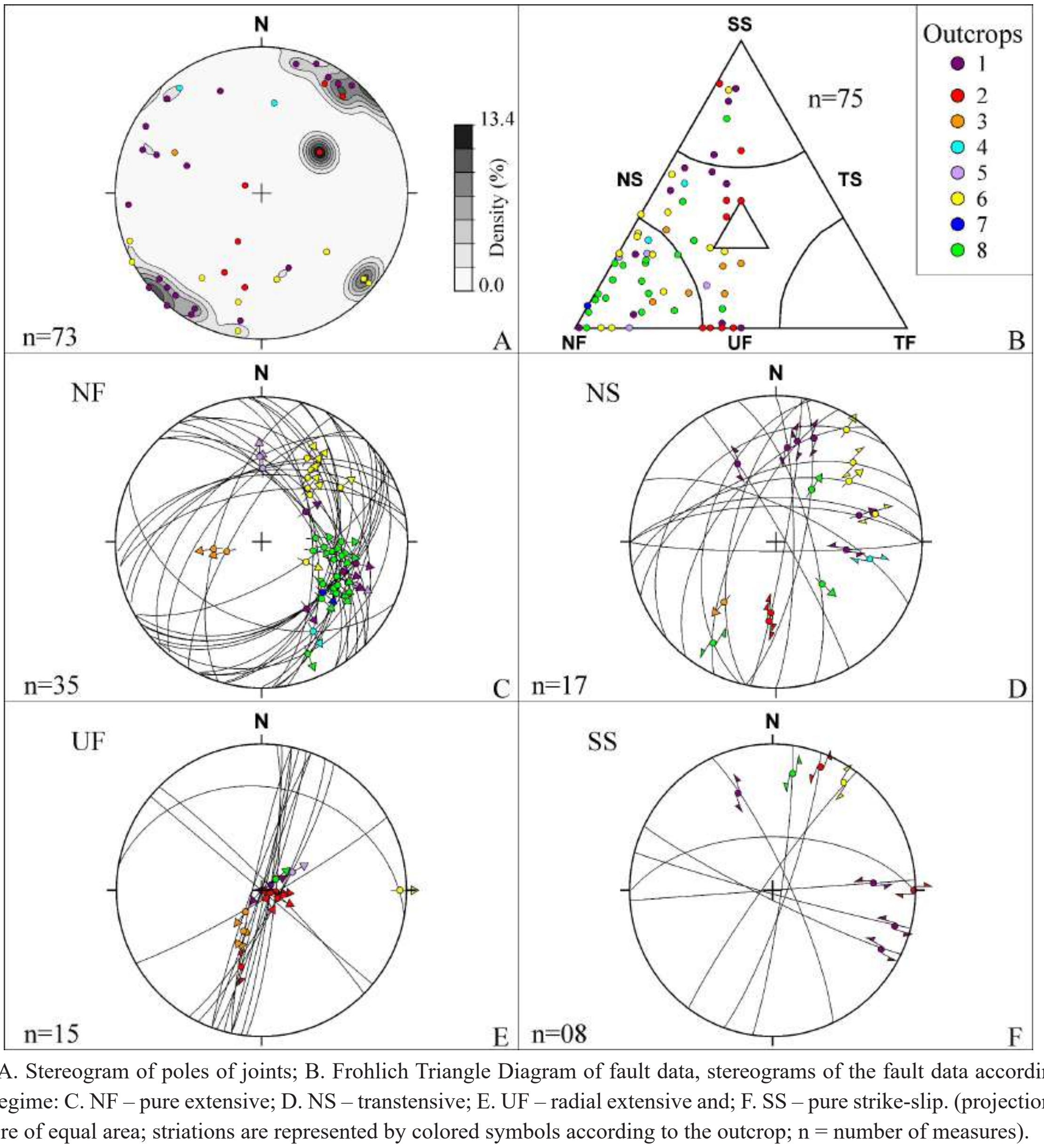

Figure 9 A. Stereogram of poles of joints; B. Frohlich Triangle Diagram of fault data, stereograms of the fault data according to the tectonic regime: C. NF – pure extensive; D. NS – transtensive; E. UF – radial extensive and; F. SS – pure strike-slip. (projections in low hemisphere of equal area; striations are represented by colored symbols according to the outcrop; n = number of measures).

The inversion and sectorization of the 75 mapped faults resulted in two different extension paleostress fields, one with NW-SE direction and the other one with NE-SW direction (Figures 10A and B). The NW-SE extensional regime is related to high-angle NE-SW normal faults, measured in outcrops 2, 3 and 8. The NE-SW regime is evidenced by oblique and transcurrent faults in the NE-SW and NW-SE directions, with striations dipping towards NE and SE, found in outcrops 1, 4 to 6, and 8.

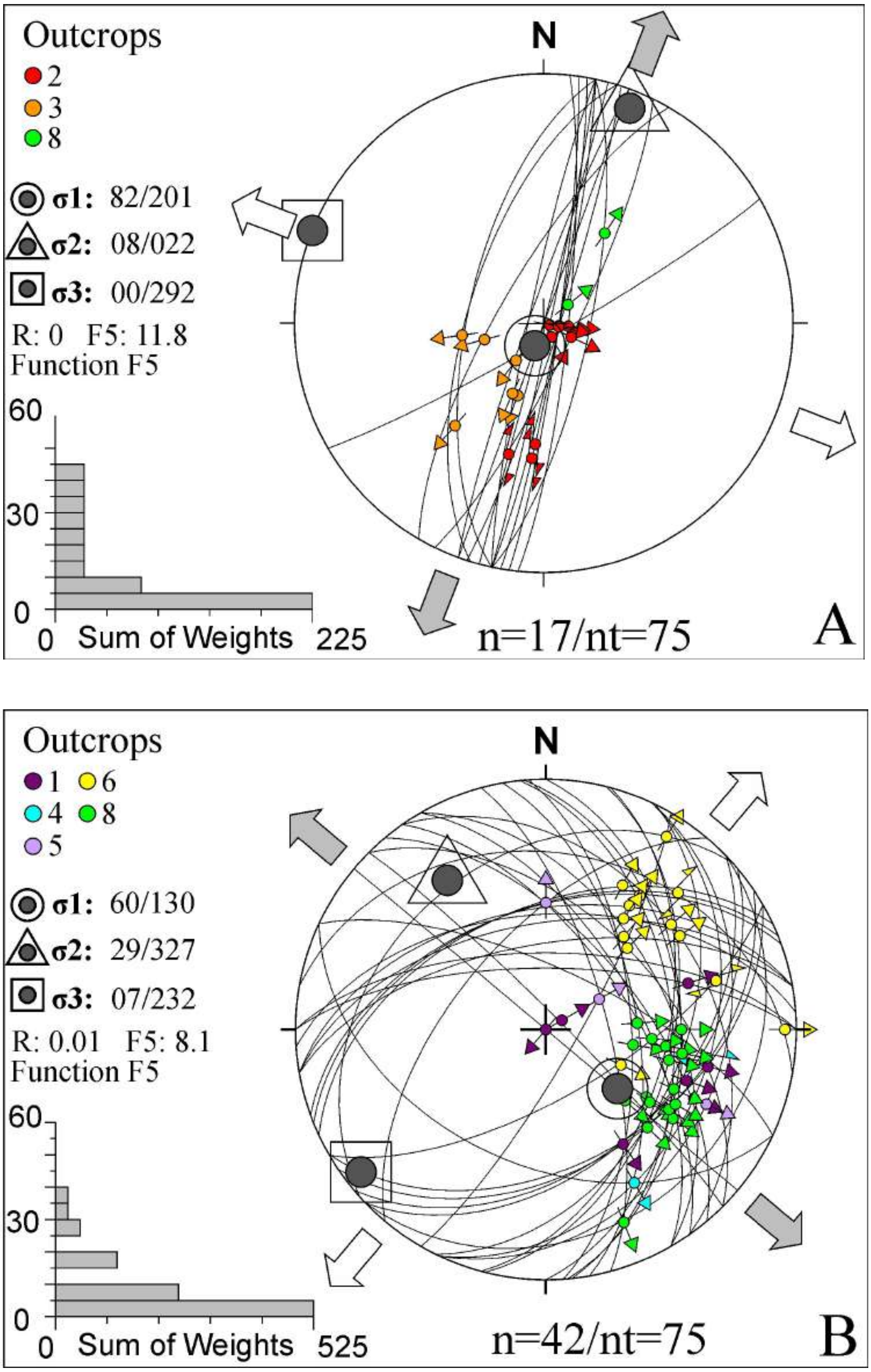

Figure 10 Paleostress regimes obtained by inversion of fault data; A. Fault data indicate extensional effort in the NW-SE and; B. extensional effort in the NE-SW. (Striations are represented by colored symbols according to the outcrop; stress axis: $\sigma_1 > \sigma_2 > \sigma_3$; n/nt = number of compatible measures/total number of measures).

5 Discussion

Field descriptions coupled with DRX analyses allow to identify birnessite, goethite, hematite, hydrobiotite, illite, kaolinite, and lithiophorite as filling materials within brittle structures, generated from weathering processes in gneisses, quartz veins and mafic dikes (Table 2).

The origin of kaolinite is closely linked to the chemical weathering of feldspars (Oberlin & Couty, 1970; Anthony *et al*., 2001), while illite originates by weathering of primary muscovite, as from the breaking of mica films in minuscule particles by physical processes until it reaches the clay-size when the primary mineral loses potassium (Velde & Meunier, 2008). Another process of illite formation is from pseudomorphic transformation of K-feldspar, during the primary stages of physical weathering (Meunier, 1980, by Velde & Meunier, 2008, p. 248). The hydrobiotite is formed in the initial stages of weathering, originated from the biotite transformation into vermiculite (Anthony *et al*., 2001; Velde & Meunier, 2008). The Fe-oxyhydroxides originate throughout the weathering process and are formed from the iron extraction of the silicate structure containing the element, during the mineral oxidation (Velde & Meunier, 2008). The presence of Mn oxides in soils indicates oxidative conditions of high pH, and are commonly associated with iron oxides such as hematite (Churchman & Lowe, 2012; Vodyanitskii *et al.,* 2004). The birnessite and lithiophorite are phyllomanganates (layer structures) that can be associated with the formation of lateritic soils, forming in the weathering initial phases of Mn-rich silicates, like the bannisterite (Anthony *et al*., 2001; Scheinost, 2004).

		Gneiss	Quartz vein	Mafic dike
		Wall-rock		
Primary Minerals	bannisterite	x		
	microcline	x		x
	muscovite	x	x	
	quartz	x	x	x
	rutile			x
	titanite			x
		Filling material		
Weathering Minerals	birnessite	x		x
	goethite	x		x
	hematite	x		x
	hydrobiotite	x		x
	illite	x	x	x
	kaolinite	x	x	x
	lithiophorite	x	x	x

Table 2 Minerals found in the filling materials and in the respective wall-rock.

The weathering minerals found in this study commonly occur distributed at different zones of a typical crystalline rock weathering profile (Righi & Meunier, 2005). The clay minerals, such as illite and kaolinite, are concentrated in the saprolite pedoplasma zone (clay-rich), although kaolinite also occurs distributed in the whole profile (Velde & Meunier, 2008). The concentration of Fe-oxyhydroxides, and consequently of Mn oxides, tends to increase towards the top of the profile, as the degree of weathering rises (Anand & Paine, 2002; Churchman & Lowe, 2012).

During the weathering processes, the accumulation of secondary minerals along brittle structures occurs from the dissolution of primary minerals by oxygenated waters and subsequent precipitation of different mineral phases in lower portions of the weathered profile. In the crystalline rock weathering profiles, these structures are found at any point of the profile (slightly altered rock, saprock, saprolite), frequently with the association of kaolinite, as the first mineral to form, and the iron oxides, that precipitate after the percolation of the fluid (Righi & Meunier, 2005). The filling materials that occur in the fault planes described here belong to this evolutionary scenario and are considered, according to the proposition of Costa (1991), as "fissure ferruginous crusts".

In the Southern Espírito Santo State, where sedimentary deposits are rare (Figure 2), the difficulties for temporal tying in studies of Cenozoic tectonics can be overcome by correlating the formation of weathering profiles in near regions, where weathering profiles have been dated. In Southeastern Brazil, some authors have dated the weathering profiles distributed along large geomorphological provinces, with decreasingly ages from the central region of the state of Minas Gerais to the coastal region of Rio de Janeiro (Carmo & Vasconcelos, 2004; Vasconcelos & Carmo, 2018; Figure 11).

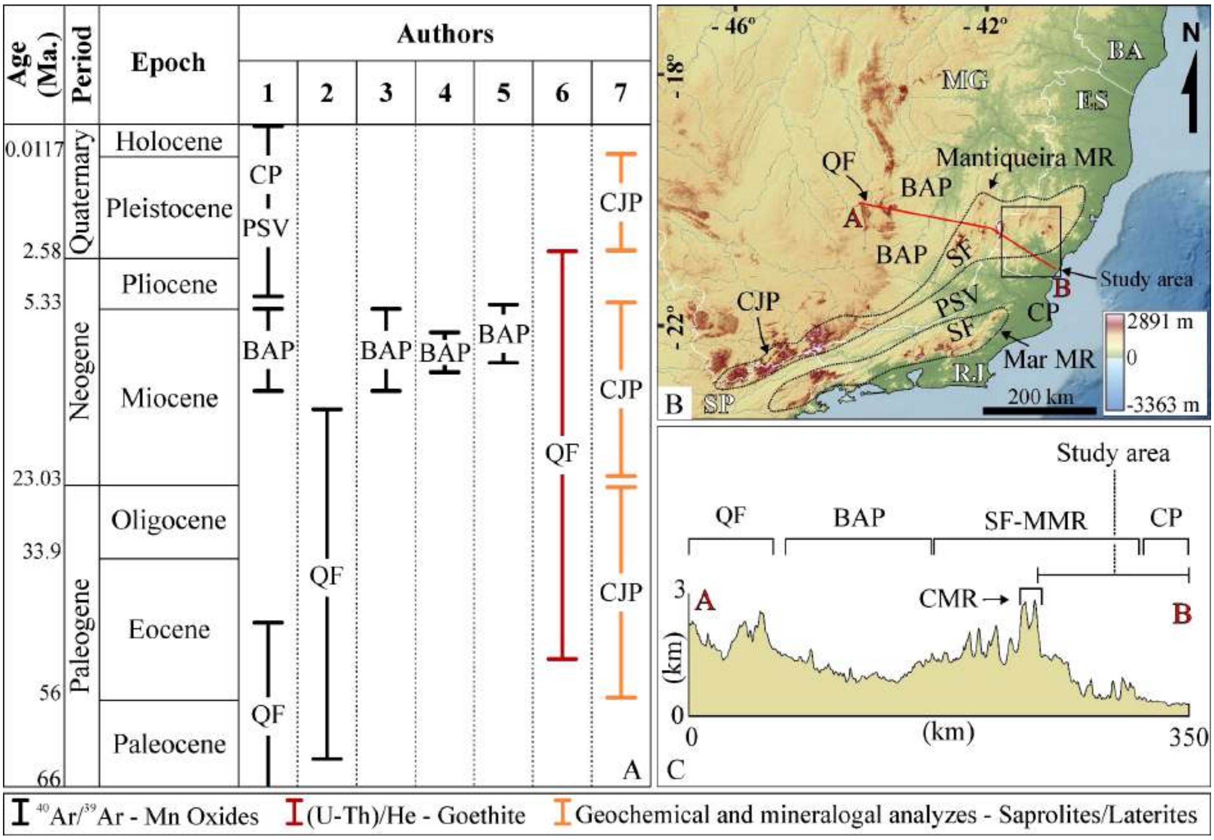

Figure 11 A. Summary table of ages attributed by previous authors for weathering profiles in the SE Brazil. 1 = Vasconcelos & Carmo (2018); 2 = Spier *et al*. (2006); 3 = Carmo & Vasconcelos (2006); 4 = Carmo & Vasconcelos (2004); 5 = Vasconcelos *et al*. (1992); 6 = Monteiro *et al*. (2014); 7 = Modenesi-Gauttieri *et al*. (2011); B. Study area and C. topographic profile in the context the main geomorphological provinces of SE Brazil. Legend: QF = *Quadrilátero Ferrífero*; BAP = Brazilian Atlantic Plateau; CJP = Campos do Jordão Plateau; SF = Scarp front; MMR = Mantiqueira Mountain Range; PSV = Paraíba do Sul Valley; CP = Coastal Plain; CMR = Caparaó Mountain Range. States: SP = São Paulo; RJ = Rio de Janeiro; ES = Espírito Santo; MG = Minas Gerais; BA= Bahia. Digital elevation mode and bathymetry from GEBCO (2020) and geomorphological provinces from Gatto *et al*. (1983), Carmo & Vasconcelos (2004) and Ross (2011).

Applying the $^{40}Ar/^{39}Ar$ method for dating Mn oxides in duricrusts and laterite deposits at *Quadrilátero Ferrífero*, Vasconcelos & Carmo (2018) and Spier *et al*. (2006) obtained ages for the mineral precipitation between 70 to 14 Ma, defining a long and well-marked history of chemical weathering favored by climatic conditions (Figures 11A and B). Monteiro *et al*. (2014), also in *Quadrilátero Ferrífero*, used the (U-Th)/He geochronological method in goethite indicating a historical process of mineral dissolution and precipitation, that would be initiated in the Eocene (48 Ma) and continued up to the Pleistocene (2 Ma). Another important Iron field in North of Brazil is the Carajás Province, in which, Shuster *et al*. (2012) dated multiple goethite formations through the (U-Th)/He method, in which precipitation occurred between the Eocene (41 Ma) and the Pleistocene (0.7 Ma).

On the Brazilian Atlantic Plateau, Vasconcelos *et al*. (1992), Carmo & Vasconcelos (2004; 2006) and Vasconcelos & Carmo (2018), also using the $^{40}Ar/^{39}Ar$ method in Mn oxides obtained ages for the formation of weathering profiles in saprolites between the Mid and Neo Miocene (13 to 5 Ma). On the Mantiqueira Mountain Range, at Campos do Jordão Plateau (São Paulo State), Modenesi-Gauttieri *et al*. (2011) consider three periods of lateritic mantle formation in saprolitic rocks: an alitization and laterite formation phase (Eocene to Late Oligocene), a monosiallitization phase (Miocene), and a podzolization phase (Pleistocene). On the Paraíba do Sul Valley and the Coastal Plain, that are close to the study area, Vasconcelos & Carmo (2018) obtained ages from weathering profiles between 4

Ma to the Present.

Cryptomelane and hollandite are the main datable minerals by the $^{40}Ar/^{39}Ar$ method in the above-cited studies. These minerals were not found at the study area, however, Carmo & Vasconcelos (2006) report that lithiophorite, mineral identified in the filling materials, occurs as microbands coating crystals of cryptomelane. Therefore, it is possible to consider that the formation of those materials, mainly in Brazilian Atlantic Plateau, Paraíba do Sul Valley and Coastal Plain, is correlated to the evolution of weathering profiles in Espírito Santo State, once the climatic conditions were supposedly similar due to the geographic proximity and the physiographic framework (Figure 11C).

Along this line of thinking, correlating the datable manganese oxides precipitation encountered in the literature - cryptomelane and hollandite - Vasconcelos *et al*. (1992), Carmo & Vasconcelos (2004; 2006), Vasconcelos & Carmo (2018); to the formation of manganese oxides found in the study area - lithiophorite and birnessite - we consider that the formation of these minerals occurred between the Miocene and the Pleistocene. Similarly, the hematite and goethite precipitation in the filling materials can be correlated to the lateritic process identified by Modenesi-Gauttieri *et al*. (2011) in São Paulo State, more probably to the phases of the lesser intensity of alteration, between the Miocene and the Pleistocene.

The weathering lateritic materials are usually considered as markers of tectonic stability phases. Tectonic movements, that occurred after these phases and printed fault marks on these materials, are newer than the lateritic materials. Then, these materials could be considered important chronological markers for the relative dating of faults.

The structural analysis of the described faults, acting after the weathering process, indicates two distensional tectonic regimes: one with the minor horizontal axis directed to NW-SE and other with this axis to NE-SW (Figure 10). This proposition fits some models from previous researchers for the Southeastern Region of Brazil. The minor tension axis to NW-SE can be related to the E-W sinistral transcurrence, acting in the Neogene, and to the NW-SE distension, that occurred in the Quaternary (as proposed by Riccomini *et al.,* 1989; Salvador & Riccomini, 1995; Silva & Mello, 2011). Another possibility is that these faults were generated by the gravitational collapse, proposed by Zalan & Oliveira (2005), which would generate a sinistral transtension with the minor axis oriented to NW-SE, between 58 and 20 Ma. The NE-SW distension can be related to a dextral transcurrence that probably acted in the Pleistocene (according to Riccomini *et al.*, 1989; Salvador & Riccomini, 1995 and Silva & Mello, 2011 models). We highlight the findings of Calegari *et al*. (2016) which affirm that, from the Neogene, ancient structures in this area were reactivated as a set of normal faults, subjected to local tension relief. These authors detach, in unison with other authors (such as Bezerra & Vita-Finzi, 2000), that the maximum horizontal axis recovered from reactivated structures can be quite different from the paleostress acting regionally.

Considering that the studied filling materials have been crystallized during the times cited above (Figure 11A) and are marked by the fault striations, we deduce that these faults were generated after the mineral precipitation, namely, after the beginning of Miocene. Probably those events occurred in tectonic pulses, with brittle structures formed in one or more extensional events. Fractures were formed and later filled with minerals newly formed by weathering; the fault striations were posteriorly printed on these filling materials in response to the movements of blocks by, at least, one subsequent extensional event. The displacement of rocky blocks would be facilitated by preexistent discontinuities and clay minerals such as illite, could be formed by dynamic metamorphism, due the comminution of the original material (muscovite) in the brittle planes, according to Velde & Meunier (2008).

These events are connected to the evolution of the Brazilian Atlantic Margin that developed since the Gondwana fragmentation, as previously studied by several authors that described the lifting and denudation processes of the Brazilian coastal margin. Some authors (e.g. Karl *et al*., 2013; Cogné *et al*., 2012; Hackspacher *et al*., 2004) affirm that such processes initiated in the Late Cretaceous and lasted until the Neogene. Similarly, in Northeastern Brazil, other authors (Jelinek *et al*., 2014; Morais Neto *et al*., 2009; Harman *et al*., 1998) placed the beginning of these events in the Early Cretaceous, persisting up to the Neogene. Anyway, the crustal lifting along the Atlantic margin led to the removal of the more ancient surficial sedimentary covers, which corroborates the idea that the weathered materials analyzed here formed with the maximum age in Miocene, as well as the faults that affected them.

6 Conclusions

The data obtained in this work permit to reach the following conclusions:

- The filling material of brittle structures found in the study area consists of primary minerals from the fresh rock and secondary minerals formed by weathering processes.

- The secondary minerals identified, the hydrobiotite, kaolinite, hematite, goethite, lithiophorite, birnessite and the illite originated by chemical weathering. The illite also can be formed by physical weathering, due to the comminution by attrition that occurs during the fault development. The mineralogical association found in the filling materials denotes the action of fluid phases with mineral precipitation at the brittle discontinuities during the weathering processes.

- The formation of the weathering minerals occurred during the Cenozoic, probably between the Miocene and the Pleistocene.

- The faults, which striations are marked on the filling materials, originated after (in the case of the manganese oxides) or during (in the case of the illite) the mineral formation, indicating that the maximum age of these faults is in the Miocene.

- The origin of the brittle structures that affected the filling materials studied here is linked to the uplifting of the Continental Brazilian Margin, when ancient geological structures were reactivated as normal faults due to the local action of an extensional regime.

7 Acknowledgments

We acknowledge National Council for Scientific and Technological Development (*Conselho Nacional de Desenvolvimento Científico e Tecnológico* - CNPq, project number 870103/2001-6, process number 141700/2018-1) for the scholarship granted to the first author, and Financier of Studies and Projects (*Financiadora de Estudos e Projetos* - FINEP, contract number 01.10.0808.00), for financial support to field works. The scientific results were obtained using Win-Tensor, software developed by Dr. Damien Delvaux, Royal Museum for Central Africa, Tervuren, Belgium. We also thanks to Prof. Dr. Adilson Viana Soares Jr, Prof. Dr. Gustavo Luiz Campos Pires and to the anonymous reviewer of Anuário do Instituto de Geociências - UFRJ for the relevant suggestions that improved this work.

8 References

Allaby, M. (ed.). 2008. *Dictionary of Earth Sciences.* 3ª Ed. Oxford, Oxford University Press. 661 p.

Alkmim F.F.; Marsak, S.; Pedrosa-Soares, A.C.; Peres, G.G.; Cruz, S.C.P. & Whittinhgton, A. 2006. Kinematic evolution of the Araçuaí-West Congo orogen in Brazil and Africa: Nutcracker tectonics during the Neoproterozoic assembly of Gondwana. *Precambrian Research, 149* (1-2): 46-64.

Almeida, F.F.M.; Hasui, Y.; Brito-Neves, B.B. & Fuck, R.A. 1981. Brazilian Structural Provinces: An Introduction. *Earth-Science Reviews, 7* (1-2): 1-29.

Anand, R.R. & Paine, M. 2002. Regolith geology of the Yilgarn Craton, Western Australia: implications for exploration. *Australian Journal of Earth Sciences*, 49: 3-162.

Angelier, J. & Mechler, P. 1977. Sur une methode graphique de recherche des contraintes principales egalement utilisables en tectonique et en seismologie: la methode des diedres droits. *Bulletin de la Société Géologique de France*, S7-XIX (6): 1309-1318.

Anthony, J.W.; Bideaux, R.A.; Bladh, K.W. & Nichols, M.C. (eds.). 2001. *Handbook of Mineralogy,* Mineralogical Society of America. USA. Available in: http://www.handbookofmineralogy.org. Accessed 30 ago 2016.

Augustin, C.H.R.R.; Lopes, M.R.S. & Silva, S.M. 2013. Lateritas: um conceito ainda em construção. *Revista Brasileira de Geomorfologia, 14* (3): 241-257.

Balsamo, F.; Bezerra, F.H.R.; Vieira, M.M. & Storti, F. 2013. Structural control on the formation of iron-oxide concretions and Liesegang bands in faulted, poorly lithified Cenozoic sandstones of the Paraíba Basin, Brazil. *Geological Society of America Bulletin, 125* (5-6): 913-931.

Bezerra, F.H.R. & Vita-Finzi, C. 2000. How active is a passive margin? Paleoseismicity in Northeastern Brasil. *Geology*, *28*: 591-594.

Brindley, G.W. & Brown, G. 1980. *Crystal Structures of Clay Minerals and Their X-ray Identification*. London, Mineralogical Society. 495 p.

Brito-Neves, B.B.; Campos Neto, M.C. & Fuck, R.A. 1999.

From Rodinia to Western Gondwana: an approach to the Brasiliano-Pan African Cycle and orogenic collage. *Episodes, 22*(3): 155-166.

Calegari, S.S.; Neves, M.A.; Guadagnin, F.; França, G.S. & Vincentelli, M.G.C. 2016. The Alegre Lineament and its role over the tectonic evolution of the Campos Basin and adjacent continental margin, Southeastern Brazil. *Journal of South American Earth Sciences, 69*: 226-242.

Carmo, I.O. & Vasconcelos, P.M. 2004. Geochronological evidence for pervasive Miocene weathering, Minas Gerais, Brazil. *Earth Surface Processes and Landforms, 29* (11): 1303-1320.

Carmo, I.O. & Vasconcelos, P.M. 2006. $^{40}Ar/^{39}Ar$ geochronology constraints on late miocene weathering rates in Minas Gerais, Brazil. *Earth and Planetary Science Letters*, *241*: 80-94.

Churchman, G.J. & Lowe, D.J. 2012. Alteration, formation and occurrence of minerals in soils. *In*: HUANG, P.M.; LI, Y. & SUMNER, M.E. (eds.). *Handbook of Soil Sciences. Properties and Processes*. CRC Press, Florida, p. 20.1-20.72.

Cogné, N.; Gallagher, K.; Cobbold, P.R.; Riccomini, C. & Gautheron, C. 2012. Post-breakup tectonics in southeast Brazil from thermochronological data and combined inverse-forward thermal history modeling. *Journal of Geophysical Research, 117*: 1-16.

Costa, M. 1991. Aspectos geológicos dos lateritos da Amazônia. *Revista Brasileira de Geociência*s, *21*(2): 146-160.

Cunningham, D.; Alkmim, F.F. & Marshak, S. 1998. A structural transect across the coastal mobile belt in the Brazilian Highlands (latitude 20°S): the roots of a Precambrian transpressional orogen. *Precambrian Research*, *92*(3): 251-275.

De Campos, C.M.; Mendes, J.C.; Ludka, I.P.; Medeiros, S.R.; Moura, J.C. & Wallfass, C. 2004. A review of the Brasiliano magmatism in southern Espírito Santo, Brazil, with emphasis on post-collisional magmatism. *Journal of the Virtual Explorer, 17*: 1-35.

De Putter, T.; Ruffet, G.; Yans, J. & Mees, F. 2015. The age of supergene manganese deposits in Katanga and its implications for the Neogene evolution of the African Great Lakes Region. *Ore Geology Reviews, 71*: 350-362.

Delvaux, D.; Moeys, R.; Stapel, G.; Petit, C.; Levi, K.; Miroshnichenko, A.; Ruzhich, V. & San'kov, V. 1997. Paleostress reconstructions and geodynamics of the Baikal region, Central Asia, Part 2. Cenozoic rifting. *Tectonophysics*, *282*: 1-38.

Delvaux, D. & Sperner, B. 2003. Stress tensor inversion from fault kinematic indicators and focal mechanism data: the TENSOR program. In: NIEUWLAND, D.A. (ed.), New Insights into Structural Interpretation and Modelling, Special Publication of the Geological Society of London, 212, p. 75-100.

Deng, X.D. & Li, J.W. 2013. 40Ar/39Ar dating of cryptomelane from the Baye manganese deposit, SW Yunnan, China: implications for growth rate of supergene Mn-oxide veins. *Science China: Earth Sciences, 59*(10): 1654-1663.

Dunn, P.J.; Leavens, P.B.; Norberg, J.A. & Ramik, R.A. 1981. Bannisterite: new chemical data and empirical fomrulae. *American Mineralogist, 66*: 1063-1067.

ERSDAC. 2013. *Earth Remote Sensing Data Analysis Center (ASTER GDEM)*. Available in: http://gdem.ersdac.jspacesystems.or.jp. Accessed 10 set 2013.

Faulkner, D.R.; Jackson, C.A.L.; Lunn, R.J.; Schlische, R.W.; Shipton, Z.K.; Wibberley, C.A.J. & Withjack, M.O. 2010. A review of recent developments concerning the structure, mechanics and fluid flow properties of fault zones. *Journal of Structural Geology, 32*(11): 1557-1575.

Féboli, W. 1993. *Programa Levantamentos Geológicos Básicos:* Folha Piúma (SF. 24-V-A-VI,), Estado do Espírito Santo, escala 1:100.000. Brasília: DNPM/ CPRM, 144 p.

Frohlich, C. 1992. Triangle diagrams: ternary graphs to display similarity and diversity of earthquake focal mechanisms. *Physics of the Earth and Planetary Interiors*, *75*: 193-198.

Fuck, R.A.; Brito-Neves, B.B. & Schobbenhaus, C. 2008. Rodinia descendants in South America. *Precambrian Research, 160*(1-2): 108-126.

Gatto, L.C.S.; Ramos, V.L.S.; Nunes, B.T.A.; Mamede, L.; Góes, M.H.B.; Mauro, C.A.; Alvarenga, S.M.; Franco, E.M.S.; Quirico, A.F. & Neves, L.B. 1983. Geomorfologia. *In*: Moreira, H.F. (ed.). Projeto RADAMBRASIL - Levantamento de Recursos Naturais: Folhas SF-23/24, Rio de Janeiro/Vitória. 32, p 305-384.

GEBCO. 2020. *General Bathymetric Chart of the Oceans*. Available in: https://www.gebco.net/data_and_products/gridded_bathymetry_data. Accessed 25 apr 2020.

GEOBASES. 2002. *Sistema Integrado de Bases Geoespaciais do Estado do Espírito Santo*. INCAPER. Available in: http://www.geobases.es.gov.br/. Accessed 28 ago 2016.

Grohmann, C.H.; Campanha, G.A.C. & Soares Junior, A.V. OpenStereo: um programa Livre e multiplataforma para análise de dados estruturais. *In:* XIII SIMPÓSIO NACIONAL DE ESTUDOS TECTÔNICOS. Campinas, 2011. *Paper*, p. 26-28.

Hackspacher, P.C.; Ribeiro, L.F.B.; Ribeiro, M.C.S.; Fetter, A.H.; Hadler Neto, J.C.; Tello, C.E.S. & Dantas, E.L. 2004. Consolidation and break-up of the South American Platform in Southeastern Brazil: tectonothermal and denudation histories. *Gondwana Research, 7*(1): 91-101.

Harman, R.; Gallagher, K.; Brown, R.; Raza, A. & Bizzi, L. 1998. Accelerated denudation and tectonic/geomorphic reactivation of the cratons of Northeastern Brazil during the Late Cretaceous. *Journal of Geophysical Research, 103* (B11): 27091-27105.

Heilbron, M.; Pedrosa-Soares, A.C.; Neto, M.C.C.; Silva, L.C.; Trow, R.A.J. & Janasi, V.A. 2004. A Província Mantiqueira. *In:* MANTESSO-NETO, V.; BARTORELLI, A.; CARNEIRO, C.D.R & BRITO-NEVES, B.B. (eds.). *Geologia do Continente Sul-Americano: evolução da obra de Fernando Flávio Marques de Almeida*. São Paulo, Becca, p. 180-212.

Horn, A.H.; Faria, B.; Gardini, G.M.; Vasconcellos, L. & Oliveira, M.R. 2007. *Programa Geologia do Brasil:* Folha Espera Feliz (SE24-V-A-IV), relatório final, escala 1:100.000. Belo Horizonte, UFMG/CPRM, 72 p.

Jelinek, A.R.; Chemale JR.F.; Van Der Beek, P.A.; Guadagnin, F.; Cupertino, J.A. & Viana, A. 2014. Denudation history and landscape evolution of the northern East-Brazilian continental margin from apatite fission-track thermochronology. *Journal of South American Earth Sciences, 54*: 158-181.

Karl, M.; Glasmacher, U.A.; Kollenz, S.; Franco-Magalhaes, A.O.B.; Stockli, D.F. & Hackspacher, P.C. 2013. Evolution of the South Atlantic passive continental margin in Southern Brazil derived from zircon and apatite (U–Th–Sm)/He and fission-track data. *Tectonophysics, 604*: 224-244.

Kurz, W.; Imber, J.; Wibberley, C.A.J.; Holdsworth, R.E. & Collettini, C. 2008. The internal structure of fault zones: fluid flow and mechanical properties. *In:* WIBBERLEY, C.A.J.; KURZ, W.; IMBER, J.; HOLDSWORTH, R.E. & COLLETTINI, C. (eds.) *The internal structure of fault zones: implications for mechanical and fluid-flow properties.* The Geological Society, London, Special publication, 299, p. 1-3.

Lourenço, F.S.; Alkmim, F.F.; Araújo, M.N.C.; Romeiro, M.A.T.; Matos, G.C. & Crósta, A.P. 2016. The Piúma lineament, southern Espírito Santo: structural expression and tectonic significance. *Brazilian Journal of Geology, 46*(4): 531-546.

Meunier, A. 2005. *Clays*. Berlin, Springer, 406 p.

Modenesi-Gauttieri, M.C.; Toledo, M.C.M; Hiruma, S.T.; Taioli, F. & Shimada, H. 2011. Deep weathering and landscape evolution in a tropical plateau. *Catena*, *85*: 221-230.

Monteiro, H.S.; Vasconcelos, P.M.; Farley, K.A.; Spier, C.A. & Mello, C.L. 2014. (U–Th)/He geochronology of goethite and the origin and evolution of cangas. *Geochimica et Cosmochimica Acta, 131*: 267-289.

Morais Neto, J.M.; Hegarty, K.A.; Karner, G.D. & Alkmim, F.F. 2009. Timing and mechanisms for the generation and modification of the anomalous topography of the Borborema Province, northeastern Brazil. *Marine and Petroleum Geology, 26*(7): 1070-1086.

Noce, C.M.; Pedrosa-Soares, A.C.; Silva, L.C. & Alkmim, F.F. 2007. O embasamento arqueano e paleoproterozóico do Orógeno Araçuaí. *Geonomos, 15*(1): 17-23.

Novo, T.A.; Noce, C.M.; Batista, G.A.P.; Quéméneur, J.J.G.; Martins, B.S.; Santos, S.W.M.; Carneiro, G.A. & Horn, A.H. 2014. *Programa Geologia do Brasil:* Geologia e Recursos Minerais da Folha Manhumirim (SF24-V-A-IV), Estados do Espírito Santo e Minas Gerais, escala 1:100.000, Belo Horizonte, CPRM, 77 p.

Oberlin, A. & Couty, R. 1970. Conditions of kaolinite formation during alteration of some silicates by water at 200°C. *Clays and Clay Minerals, 18*: 347-356.

Pedrosa-Soares, A.C.; Campos, C.; Noce, C.M.; Silva, L.C.; Roncato, J.; Novo, T.; Medeiros, S.; Castañeda, C.; Queiroga, G.; Dantas, E.; Dussin, I. & Alkmim, F.F. 2011. Late Neoproterozoic-Cambrian granitic magmatism in the Araçuaí Orogen, the Eastern Brazilian Pegmatite Province and related mineral resources (SE Brazil). *Journal of the Geological Society of London, 350*: 25-51.

Pedrosa-Soares, A.C.; Alkmim, F.F.; Tack, L.; Noce, C.M; Babinski, M.; Silva, L.C. & Martins-Neto, M.A. 2008. Similarities and differences between the Brazilian and African counterparts of the Neoproterozoic Araçuaí-West Congo Orogen. *Journal of the Geological Society of London, 294*: 153-172.

Pedrosa-Soares, A.C.; Noce, C.M.; Alkmim, F.F.; Silva, L.C.; Babinski, M.; Cordani, U. & Castañeda, C. 2007. Orógeno Araçuaí: síntese do conhecimento 30 anos após Almeida 1977. *Geonomos, 15*(1): 1-16.

Pedrosa-Soares, A.C.; Noce, C.M.; Wiedemann, C.M. & Pinto, C.P. 2001. The Araçuaí-West-Congo Orogen in Brazil: an overview of a confined orogen formed during Gondwanaland assembly. *Precambrian Research, 110*(1-4): 307-323.

Pedrosa-Soares, A.C. & Wiedemann-Leonardos, C.M. 2000. Evolution of the Araçuaí Belt and its connection to the Ribeira Belt, Eastern Brazil. *In:* CORDANI U.G.; MILANI, E.J.; TOMAZ FILHO, A. & CAMPOS, D.A. (eds.). *Tectonic Evolution of South America.* São Paulo, Sociedade Brasileira de Geologia, p. 265-285.

Riccomini, C.; Peloggia, A.U.G.; Saloni, J.C.L.; Kohnke, M.W. & Figueira, R.M. 1989. Neotectonic activity in the Serra do Mar rift system (southeastern Brazil*). Journal of South America Earth Sciences*, *2*(2): 191-197.

Righi, D & Meunier, A. 1995. Origin of Clays by Rock Weathering and Soil Formation. *In:* VELDE, B. (ed.) *Origin and mineralogy of clays. Clays and the environment*. Springer, Berlin, p. 43-161.

Romano, A.W. & Castañeda, C. 2006. A tectônica distensiva pós-mesozoica no condicionamento dos depósitos de bauxita da mata mineira. *Geonomos, 14*(1-2): 1-5.

Ross, J. 2011. Relevo brasileiro: uma nova proposta de classificação. *Revista do Departamento de Geografia*, *4*: 25-39.

Salvador, E.D. & Riccomini, C. 1995. Neotectônica da região do alto estrutural de Queluz (SP-RJ, Brasil). *Revista Brasileira de Geociências*, *25*(3): 151-164.

Santos, M. & Ladeira, F.S.B. 2006. Tectonismo em perfis de alteração da Serra de Itaqueri (SP): Análise através de indicadores cinemáticos de falhas. *Geociências, 25*(1): 135-149.

Scheinost, A.C. 2004. Metal Oxides. In: HILLEL, D (ed.). *Encyclopedia of Soils in the Environment.* Elsevier, 2, p. 428-438.

Shuster, D.L.; Farley, K.A.; Vasconcelos, P.M.; Balco, G.; Monteiro, H.S.; Waltenberg, K. & Stone, J.O. 2012. Cosmogenic ^{3}He in hematite and goethite from Brazilian "canga" duricrust demonstrates the extreme stability of these surfaces. *Earth and Planetary Science Letters, 329-330*: 41-50.

Silva, L.C.; Mcnaughton, N.J.; Armstrong, R.; Hartmann, L.A. & Fletcher, I.R. 2005. The Neoproterozoic Mantiqueira Province and its African connections: a zircon-based U–Pb geochronologic subdivision for the Brasiliano/Pan-African systems of orogens. *Precambrian Research, 136*(3-4): 203-240.

Silva, M.A.; Camozzato, E.; Paes, V.J.C.; Junqueira, P.A. & Ramgrab, G.E. Folha SF.24-Vitoria. 2004. SCHOBBENHAUS, C.; GONÇALVES, J.H.; SANTOS, J.O.S.; ABRAM, M.B.; LEÃO NETO, R.; MATOS, G.M.M.; VIDOTTI, R.M.; RAMOS, M.A.B. & JESUS, J.D.A. (eds.), 2004. *Carta Geológica do Brasil ao Milionésimo***,** Sistema de Informações Geográficas. Programa Geologia do Brasil. Brasília, CPRM.

Silva, T.P. & Mello, C.L. 2011. Reativações Neotectônicas na Zona de Cisalhamento do Rio Paraíba do Sul (Sudeste do Brasil). *Geologia USP. Série Científica,* 11(1): 95-111.

Spier, C.A.; Vasconcelos, P.M. & Oliveira, S.M.B. 2006. ^{40}Ar/^{39}Ar geochronological constraints on the evolution of lateritic iron deposits in the Quadrilátero Ferrífero, Minas Gerais, Brazil. *Chemical Geology, 234*(1-2): 79-104.

Vasconcelos. P.M.; Becker, T.A; Renne, P.R & Brimhal, G.H. 1992. Age and duration of weathering by ^{40}K-^{40}Ar and ^{40}Ar/^{39}Ar analysis of potassium-manganese oxides. *Science*, 258: 451-455.

Vasconcelos, P.M. & Carmo, I.O. 2018. Calibrating denudation chronology through ^{40}Ar/^{39}Ar weathering geochronology. *Earth-Science Reviews*, *179*: 411-435.

Velde, B. & Meunier, A. 2008. *The Origin of Clay Minerals in Soils and Weathered Rocks.* Berlim, Springer, 406 p.

Vieira, V.S. & Menezes, R.G. (org.). 2015. *Geologia e Recursos Minerais do Estado do Espírito Santo:* texto explicativo do mapa geológico e de recursos minerais, escala 1:400.000. Belo Horizonte, CPRM, 289 p.

Vodyanitskii, Y.N.; Vasil'ev, A.A.; Lesovaya, S.N.; Sataev, E.F & Sivtsov, A.V. 2004. Formation of Manganese Oxides in Soils. *Eurasian Soil Science*, *37*(6): 572-584.

Wiedemann, C.M.; Campos, C.M.; Medeiros, S.R.; Mendes, J.C.; Ludka, I.P. & Moura, J.C. 2002. Architecture of Late orogenic plutons in the Araçuaí-Ribeira Folded Belt, Southeast Brazil. *Gondwana Research, 19*: 381-399.

Zalán, P.V. & Oliveira, J.A.B. 2005. Origem e evolução do Sistema de Riftes Cenozóicos do Sudeste do Brasil. *Boletim de Geociências da Petrobras*,*13*(2): 269-300.

Zhang, Y.; Schaubs, P.M.; Zhao, C.; Ord, A. Hobbs, B.E. & Barnicoat, A.C. 2008. Fault-related dilation, permeability enhancement, fluid flow and mineral precipitation patterns: numerical models. *In:* WIBBERLEY, C.A.J.; KURZ, W.; IMBER, J.; HOLDSWORTH, R.E. & COLLETTINI, C. (eds.). *The Internal Structure of Fault Zones: implications for mechanical and fluid-flow properties.* The Geological Society, London, 299, p. 239-255.